

First-order phase transitions in the Montorsi-Rasetti model

K. Michielsen and H. De Raedt

*Institute for Theoretical Physics and Materials Science Centre, University of Groningen, Nijenborgh 4,
NL-9747 AG Groningen, The Netherlands*

(Received 19 April 1994)

Exact diagonalization and quantum Monte Carlo methods are used to explore the zero-temperature phase diagram of a simplified Hubbard model extended with bond-charge–site-charge interactions. Numerical results for the grand potential and for its first derivatives with respect to the Coulomb potential and the chemical potential strongly suggest the occurrence of first-order phase transitions. It is shown that there is a close analogy between the first-order ground-state phase transitions in this quantum system and the phase transitions in classical (P, V, T) systems.

PACS number(s): 05.30.Fk, 71.30.+h

I. INTRODUCTION

The study of critical phenomena in quantum systems heavily draws on analogies with classical statistical mechanics. For continuous phase transitions, i.e., phase transitions accompanied by a continuous change of state [1], the connection between the critical properties of the classical system at $T > 0$ and the critical $T = 0$ behavior of the corresponding quantum system is well known. Suzuki has shown how to express the partition function of a d -dimensional quantum spin system as a partition function of a $(d + 1)$ -dimensional Ising model with many-spin interactions [2]. This equivalence was used to prove rigorously the conjecture [3] that the singularities in the thermodynamic functions of the $(d + 1)$ -dimensional Ising model (with nearest-neighbor interactions only) are in one-to-one correspondence to singularities in the ground-state properties of the d -dimensional Ising model with a transverse magnetic field [2]. Also, the critical behavior of the ground state of the one-dimensional (1D) $S = \frac{1}{2}$ XY model in a magnetic field is the same as that of the two-dimensional (2D) Ising model at the critical temperature [4]. A path-integral treatment of the 1D $S = 1$ XY model with single-ion anisotropy, in combination with renormalization-group arguments, indicates that at criticality the quantum system belongs to the same universality class as the 2D planar rotator (XY) model [5]. Heuristic arguments [6] suggest that for $T > 0$ quantum-mechanical models fall into the same universality class as their classical counterparts, leading to the same critical exponents, etc.

In this paper we study a many-body quantum model that exhibits $T = 0$ phase transitions that cannot be associated with a continuous change of state of the system. The model studied is the simplified Hubbard model [7] extended with bond-charge–site-charge interactions. The simplified Hubbard model itself can be interpreted as a model for an annealed binary alloy, for crystallization [8,9], or to study mixed valence states in rare-earth compounds [10]. The bond-charge–site-charge interaction is an off-diagonal part of the Coulomb interaction which leads to a (dis)continuous metal-insulator transition at

half-filling [11].

The paper is organized as follows. In Sec. II we specify the model Hamiltonian and discuss its basic properties. Results for the ground-state energy and other physical quantities are presented in Sec. III, where we also discuss how the $T = 0$ phase transitions that occur in the quantum model are related to conventional phase transitions [1] provided a proper identification of the state variables is made. Different views of the three-dimensional phase diagram, given in Sec. IV, summarize our results.

II. MODEL

We will investigate the ground-state properties of the Montorsi-Rasetti model [12], defined by the Hamiltonian

$$\begin{aligned} \mathcal{H} &= \mathcal{H}_1 + \mathcal{H}_2, \\ \mathcal{H}_1 &= \frac{t}{2} \sum_{\langle i,j \rangle} \sum_{\sigma, \sigma'} (a_{i,\sigma}^\dagger a_{j,\sigma'} + \text{H.c.}) \\ &\quad - \frac{t'}{2} \sum_{\langle i,j \rangle} \sum_{\sigma, \sigma'} (a_{i,\sigma}^\dagger a_{j,\sigma'} + \text{H.c.}) \\ &\quad \times (n_{i,-\sigma} + n_{j,-\sigma'} - \gamma n_{i,-\sigma} n_{j,-\sigma'}), \\ \mathcal{H}_2 &= -\mu \sum_i \sum_{\sigma} n_{i,\sigma} + U \sum_i n_{i,\uparrow} n_{i,\downarrow}. \end{aligned} \quad (2.1)$$

Here $a_{i,\sigma}^\dagger$ and $a_{i,\sigma}$ are the creation and annihilation operators, respectively, for an electron with spin $\sigma = \uparrow, \downarrow$ at lattice site i , $n_{i,\sigma}$ denotes the number operator at site i , and the sum $\langle i, j \rangle$ is over distinct pairs of nearest-neighbor lattice sites on a d -dimensional hypercubic lattice with periodic boundaries and of linear size L . t is the hopping parameter, t' is the bond-charge–site-charge interaction, U is the on-site Coulomb interaction, μ is the chemical potential, and γ is a real number that controls the relative amplitude of the allowed hopping processes. If $t' = t$, \mathcal{H}_1 and \mathcal{H}_2 commute so that the total number of doubly occupied sites is a conserved quantity [12].

Exact diagonalization and quantum Monte Carlo (QMC) simulations have shown that for $t' = t$, at $T = 0$ and for dimensions $d = 1, 2, 3$, model (2.1) exhibits a Mott

metal-insulator transition as a function of U [13,14]. A discussion of the relation of the Montorsi-Rasetti model to the Hubbard [15,16] and simplified Hubbard models [8,15,17], the Falicov-Kimball model [10], and the Hirsch model [18], as well as an extensive account of the static and dynamic properties of Hamiltonian (2.1) for the case $t'=t$ can be found in Refs. [11,13].

Introducing new fermion operators [12]

$$A_i = \frac{1}{\sqrt{2}}(a_{i,\uparrow} + a_{i,\downarrow}), \quad (2.2a)$$

$$B_i = \frac{1}{\sqrt{2}}(a_{i,\uparrow} - a_{i,\downarrow}), \quad (2.2b)$$

$$M_{ij} = \begin{cases} UD_i - \mu, & \text{if } i=j. \\ t - t'(D_i + D_j - \gamma D_i D_j), & \text{if } i \text{ and } j \text{ are nearest neighbors;} \\ 0, & \text{otherwise.} \end{cases} \quad (2.4)$$

As $[D_i, A_j] = [D_i, A_j^\dagger] = 0$ for all i and j , expression (2.4) shows that the eigenstates of Hamiltonian (2.3) are also eigenstates of the number operators D_i [12]. Accordingly, the B_i fermions cannot move. We will call these fermions the immobile particles, in contrast to the mobile particles represented by the operators A_i and A_i^\dagger .

For each set of eigenvalues $\{s_i = 0, 1\}$ of the D_i 's Hamiltonian (2.3) is a quadratic form of the fermion operators (A_i^\dagger, A_i) , hence the eigenstates of the many-particle system are simply products of the single-particle eigenstates. The latter are obtained by diagonalizing the $L \times L$ matrix M for each of the 2^{dL} configurations of the s_i 's. For systems containing up to 16 sites the results presented below are numerically exact. For larger systems, a QMC method is used to compute the expectation values of observables [19]. For the present purposes, the QMC technique only serves to make sure that certain steplike structures that appear in the figures are finite-size effects. It turns out that finite-size effects are easy to recognize and that it is straightforward to account for them. Unless the QMC data is revealing different physics, it will be omitted for the sake of clarity. Furthermore, we will only present results for one-dimensional systems because exact and QMC calculations demonstrate that the $T=0$ phase transitions in the model do not depend on the dimensionality of the lattice [14]. The lattice dimensionality is also not a relevant parameter for most other model properties [14].

III. RESULTS

We will investigate the behavior of the grand potential per site at $T=0$,

$$\Omega = - \lim_{\rho \rightarrow \infty} \frac{1}{\beta L^d} \ln \text{Tr} e^{-\beta \mathcal{H}} = L^{-d} \langle \mathcal{H} \rangle, \quad (3.1)$$

as a function of the model parameters U , and the density

$$n = N + D, \quad (3.2)$$

and denoting the corresponding number operators by

$$N_i = A_i^\dagger A_i, \quad (2.2c)$$

and

$$D_i = B_i^\dagger B_i, \quad (2.2d)$$

Hamiltonian (2.1) can be written as

$$\mathcal{H} = \sum_{i,j} A_i^\dagger M_{ij} A_j - \mu \sum_i D_i, \quad (2.3)$$

where

where

$$N = \frac{1}{L^d} \sum_i \langle N_i \rangle, \quad (3.3)$$

and

$$D = \frac{1}{L^d} \sum_i \langle D_i \rangle, \quad (3.4)$$

for various t' (we use units such that $t=1$). For simplicity, we will set $\gamma=2$ such that the system is invariant for particle-hole symmetry [11]. The average double occupancy per site will be denoted by

$$P = \frac{1}{L^d} \sum_i \langle N_i D_i \rangle. \quad (3.5)$$

Numerical results for $n = n(\mu)$ for the case $t'=t$ are given in Fig. 1. For each curve U is kept constant. The small steps are finite-size effects and disappear if the sys-

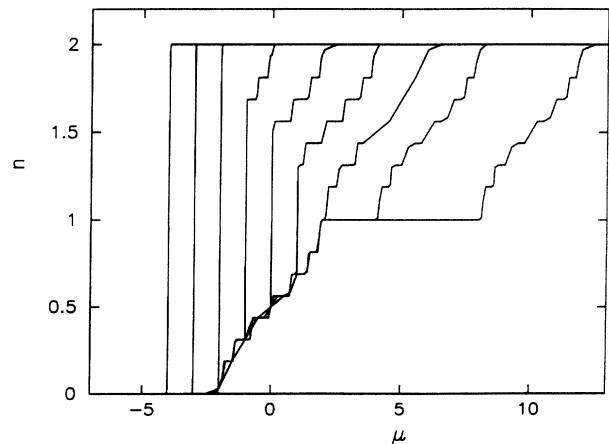


FIG. 1. n as a function of μ for a ring of 16 sites for $t'=t=1$, $\gamma=2$, and $\beta=100$. From left to right: $U = -8, -6, -4, -2, 0, 2, 4, 6$, and 10 .

tem is made larger (QMC data are not shown). From Fig. 1 it follows that there are three different regimes, depending on the value of U .

For $U \leq -4$ the system is known to be a nonmagnetic insulator [14]. In Fig. 2 we present typical results for the grand potential Ω , the density n , and the average double occupancy per site P in this regime. Taking, for example, $U = -8$, Fig. 2(a) shows that Ω is a concave function of μ , as expected [1]. There is a bend in the curve at $\mu = U/2$. By symmetry, for this value of μ , the density $n = 1$ [14]. At constant U (e.g., $U = -8$), very small changes in μ result in large changes in the density, as exemplified in Fig. 2(b). The fact that $\partial\mu/\partial n|_{\mu=U/2}$ is nonzero is due to finite-size effects. In the region where $\partial\mu/\partial n|_{\mu=U/2} \approx 0$ two phases coexist. For $\mu \leq -4.05$, $n = 0$ and $D = 0$, and hence there are no particles in the system. On the other hand, for $\mu \geq -3.95$, $n = 2$ and $D = 1$, and all the particles form pairs. Exact calculations for the canonical ensemble (results not shown) demonstrate that for an even number of particles the immobile particles are distributed randomly over the lattice. For $U \leq -4$, $P = n/2$ and all mobile particles pair with the immobile ones [13,14]. Therefore, precisely at half-

filling, the ground state is 2^{dL} times degenerate. For $n < 1$ and an odd number of particles, $D = N - 1$ and all immobile particles occupy one part of the lattice. Since all mobile particles pair with the immobile ones ($P = n/2$), this results in a lattice of which one part is occupied by pairs of particles and another part that contains only one mobile particle. For $n > 1$ interchanging particles and holes leads to a similar conclusion. These results suggest that in the regime $U \leq -4$ the system exhibits phase separation between a phase with no particles and a phase where all sites are filled with pairs of particles. At $U = 2\mu$, the two phases coexist.

Additional evidence for a first-order phase transition is presented in Figs. 2(c) and 2(d). For fixed μ ($\mu = -4$ in this example), the grand potential is a concave function of U and has a bend at $U = 2\mu$. The presence of the bend is reflected by the jump of the double occupancy as a function of U [see Fig. 2(d)]. Thus for fixed μ the system exhibits a first-order phase transition as a function of U .

It is instructive to compare Figs. 2(a)–2(d) with plots of the typical behavior for the Gibbs free energy and its first derivatives at a first-order phase transition in a classical (P, V, T) system (see, e.g., Ref. [1], p. 88). If we

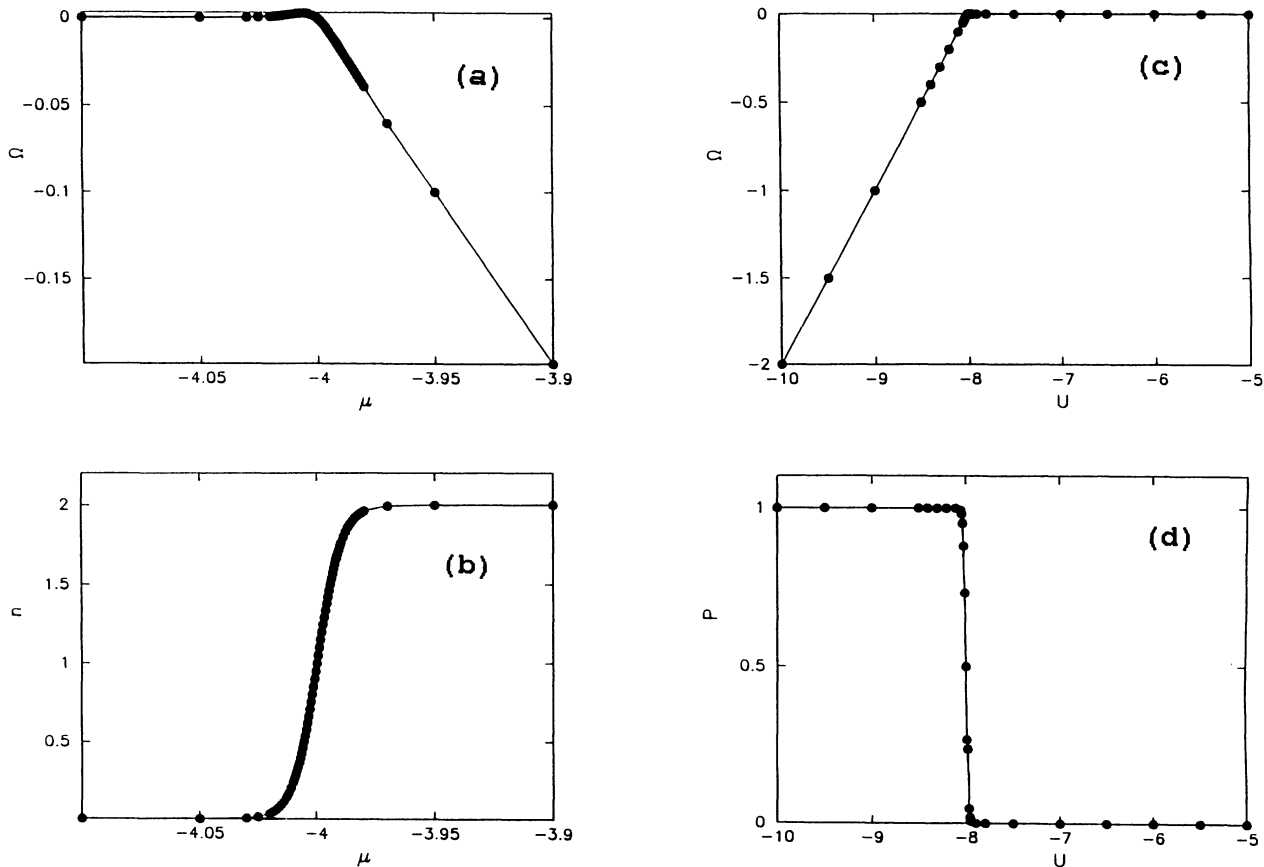


FIG. 2. Grand potential and first derivatives with respect to μ and U as a function of μ and U , respectively, for a ring of 16 sites for $t' = t = 1$, $\gamma = 2$, and $\beta = 100$. (a) Ω as a function of μ for $U = -8$; (b) $n = -\partial\Omega/\partial\mu|_U$ as a function of μ for $U = -8$; (c) Ω as a function of U for $\mu = -4$; (d) $P = \partial\Omega/\partial U|_\mu$ as a function of U for $\mu = -4$. The lines are guides to the eye.

identify

$$\Omega(\mu, U) \equiv \text{Gibbs free energy}, \quad (3.6a)$$

$$\mu \equiv \text{Pressure}, \quad (3.6b)$$

$$U \equiv \text{Temperature}, \quad (3.6c)$$

it is clear that there is a close analogy between the $T=0$ phase transition in the quantum model studied here and the first-order phase transition in a classical system at $T>0$. Note that the jump of the double occupancy in the quantum model corresponds to the latent heat of the transition in the classical system.

Additional support for this equivalence is given in Fig. 3, where we show results for $|U| < 4$. In this regime the system is a metal [14]. Figure 3(a) depicts Ω as a function of μ at constant U ($U=-2$ in this example). Ω is a monotonically decreasing function of μ and has a bend at $\mu=U/2$. The two different nonzero slopes at the bend indicate that, in contrast to the previous case $U \leq -4$, the density will not jump between zero and 2. Indeed, Fig. 3(b) shows that, except for $\mu \approx U/2$, the density n varies smoothly with μ . The small steplike structures in $n=n(\mu)$ are due to finite-size effects. For $\mu \neq U/2$, $\partial\mu/\partial n|_U > 0$ and hence the system is in a stable state.

When $\mu < U/2$, $D=0$ and $N>0$, i.e., there are only mobile particles in the system. On the other hand, for $\mu > U/2$, $N>0$ and $D=1$, so that each lattice site is occupied by an immobile particle. At $\mu=U/2$, $\partial\mu/\partial n|_U=0$ and the two phases, characterized by $D=0$ and $D=1$, respectively, coexist.

According to our interpretation above we expect the grand potential Ω and the double occupancy P to exhibit the behavior characteristic of a first-order phase transition and, indeed, as shown in Figs. 3(c) and 3(d), this is the case. At constant μ ($\mu=-1$ in this example), Ω increases with U for $U < 2\mu$ and is constant otherwise [see Fig. 3(c)]. It has a bend at $U=2\mu$ and this bend corresponds to the jump in the P vs U plot [see Fig. 3(d)]. Clearly a nonzero P requires $D > 0$ so we must enter a regime where immobile particles are present. Once we are in this regime, P increases smoothly because of the increasing number of mobile particles. The "plateau" in $P=P(U)$ [see Fig. 3(d)] is only a finite-size effect. Apparently, also, these results are in concert with our interpretation in terms of a first-order $T=0$ phase transition.

For $U > 4$ and $n \neq 1$ the system is a metal whereas for $n=1$ it is an insulator [14]. For fixed U , $n=n(\mu)$ exhibits a plateau at $n=1$ (see Fig. 1). For $n \neq 1$ the density changes smoothly with μ (if we disregard finite-size

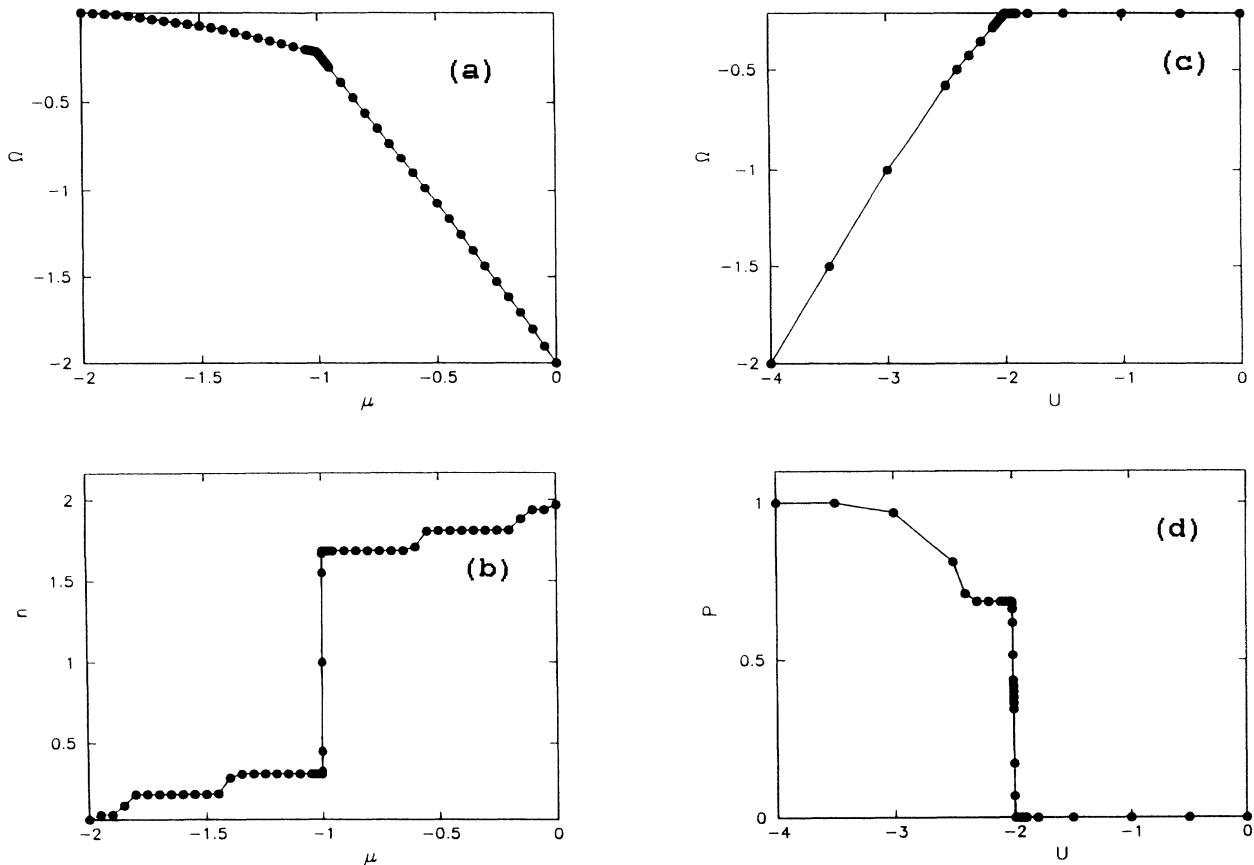


FIG. 3. Grand potential and first derivatives with respect to μ and U as a function of μ and U , respectively, for a ring of 16 sites for $t'=t=1$, $\gamma=2$, and $\beta=100$. (a) Ω as a function of μ for $U=-2$; (b) $n = -\partial\Omega/\partial\mu|_U$ as a function of μ for $U=-2$; (c) Ω as a function of U for $\mu=-1$; (d) $P = \partial\Omega/\partial U|_\mu$ as a function of U for $\mu=-1$. The lines are guides to the eye.

effects). Hence the system does not phase separate if $U > 4$.

The first-order phase transitions described above persist if $0 < t' < 2t$. As in the $t' = t$ case, at half-filling and $T = 0$ there is a Mott metal-insulator transition at the critical coupling $U_c = U_c(t')$ [11]. Unlike for $t' = t$, the metal-insulator transition is discontinuous, i.e., with increasing U the gap in the density of states opens abruptly at the metal-insulator transition point U_c [11]. For $\gamma = 2$ and $0 < t' < 2t$ there are at most three regimes with different physical behavior, namely, $U \leq -U_c$, $|U| < U_c$, and $U \geq U_c$, corresponding to an insulator, a metal, and an insulator (if $n = 1$), respectively [11].

For $|U| < U_c$, the salient features of the ground-state phase transitions are the same as in the case $t' = t$. New features appear if $U \leq -U_c$ and $U \geq U_c$. For $U \leq -4$, as, for example, shown in Fig. 4 for $t' = 0.5$ and $U = -6$ ($|U_c| = 3$), Ω is a concave function of μ but instead of having one bend, it now displays two. From Fig. 4(b) it follows that these bends define a small range of μ values for which the system is half-filled ($n = 1$); this is in contrast to the $t' = t$ case [compare with Fig. 2(b)]. In this regime the immobile particles order into a two-sublattice (bipartite) configuration with one sublattice completely

occupied and the other completely empty (chessboard configuration). Since for $U \leq -4$, $P \approx \frac{1}{2}$, most of the mobile particles pair with the immobile ones [11]. Away from this regime calculations for a fixed number of particles (results not shown) demonstrate that for an even number of particles the immobile particles order periodically with maximum possible spacing between them. Since for $U \leq -4$, $P \approx n/2$, most mobile particles pair with the immobile ones [11]. For $n < 1$ and an odd number of particles $D = N - 1$ and all immobile particles order into a chessboard configuration in one part of the lattice. Since most of the mobile particles pair with the immobile ones ($P \approx n/2$), this results in a lattice of which one part is occupied by pairs of particles ordered in a nearly perfect chessboard configuration and another part is pair free. For $n > 1$ interchanging particles and holes leads to a similar conclusion. A plot of Ω as a function of U for fixed μ ($\mu = -3$ in this example) is given in Fig. 4(c). The position of the two bends in Ω vs U correspond to the values of U at which the double-occupancy P makes a jump [see Fig. 4(d)]. Figures 4(b) and 4(d) might give the impression that n (respectively, P) is changing smoothly, but analysis of QMC data (not shown) indicates that this is not the case. The apparent smoothness

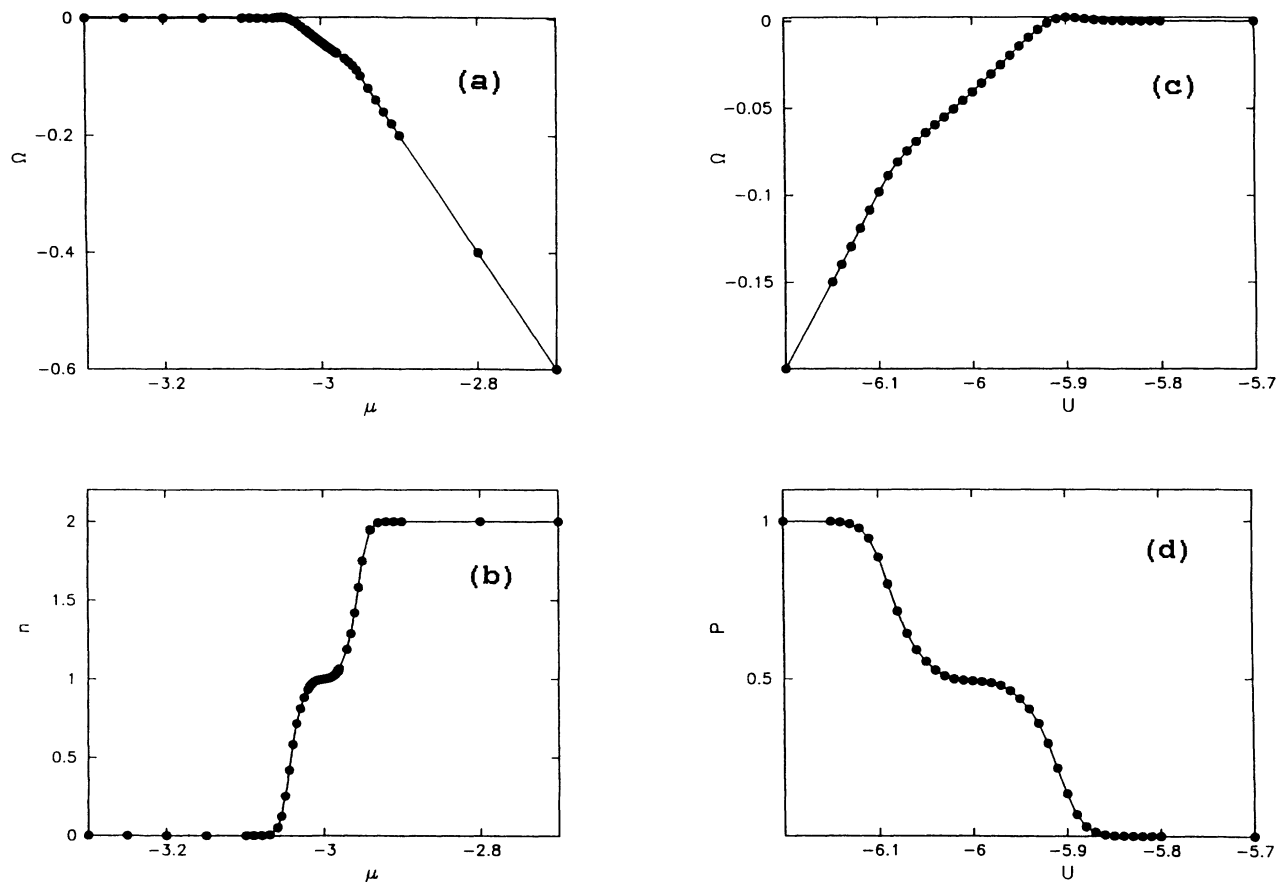


FIG. 4. Grand potential and first derivatives with respect to μ and U as a function of μ and U , respectively, for a ring of 16 sites for $t = 1$, $t' = 0.5$, $\gamma = 2$, and $\beta = 100$. (a) Ω as a function of μ for $U = -6$; (b) $n = -\partial\Omega/\partial\mu|_U$ as a function of μ for $U = -6$; (c) Ω as a function of U for $\mu = -3$; (d) $P = \partial\Omega/\partial U|_\mu$ as a function of U for $\mu = -3$. The lines are guides to the eye.

disappears if the system size increases. These results suggest that in the regime $U \leq -4$ and $n < 1$ ($n > 1$) the system exhibits phase separation between a phase with no particles (a phase where all sites are filled with pairs of particles) and a phase where pairs of particles are ordered into a nearly perfect chessboard configuration. This is the case for all $t' \neq t$ (see, for example, the results for $t' = 0$ in Ref. [20]).

For fixed $-4 < U \leq -U_c$ (results not shown), $n = n(\mu)$ exhibits a small plateau of size Δ at $n = 1$. For this small range of μ values the immobile particles are ordered into a chessboard configuration. When $\mu < (U - \Delta)/2$, $D = 0$ and $N > 0$, i.e., there are only mobile particles in the system. At $\mu = (U - \Delta)/2$, $\partial\mu/\partial n|_U = 0$ and the two phases characterized by $D = 0$ and a nearly perfect chessboard configuration of pairs of particles coexist. On the other hand, for $\mu > (U + \Delta)/2$, $N > 0$ and $D = 1$, so that each lattice site is occupied by an immobile particle. At $\mu = (U + \Delta)/2$, $\partial\mu/\partial n|_U = 0$, so that now the two phases characterized by $D = 1$ and a nearly perfect chessboard configuration of pairs of particles coexist. Similar behavior is found if $t' \leq 0$ or $t' \geq 2t$ and $-4 < U < 0$.

For $U \geq U_c$, an example being shown in Fig. 5 for the case $t' = 0.2$ and $U = 6$ ($|U_c| = 1.8$), Ω displays two bends as a function of μ defining a range Δ of μ values for

which the system is half-filled. In this regime the immobile particles order into a chessboard configuration. Since for $U \geq U_c$, $P \approx 0$, most of the mobile particles fill in the empty places of the chessboard configuration formed by the immobile particles [11]. The three different nonzero slopes at the bends indicate that, in contrast to the case $U \leq -4$, the density will not jump between 0, 1, and 2. Indeed, Fig. 5(b) shows that, except for $\mu \approx (U \pm \Delta)/2$, the density n varies smoothly with μ (apart from finite-size effects). When $\mu < (U - \Delta)/2$, $D = 0$ and $N > 0$. At $\mu = (U - \Delta)/2$, $\partial\mu/\partial n|_U = 0$ and the two phases characterized by $D = 0$ and a nearly perfect chessboard configuration of unpaired mobile and immobile particles ($P \approx 0$) coexist. On the other hand, for $\mu > (U + \Delta)/2$, $D = 1$ and $N > 0$. At $\mu = (U + \Delta)/2$ the two phases characterized by $D = 1$ and a nearly perfect chessboard configuration of unpaired mobile and immobile particles ($P \approx 0$) coexist. These features are also present if $t' \leq 0$ or $t' \geq 2t$ and $U > 0$. A plot of Ω vs U for fixed μ ($\mu = 3$ in this example) is given in Fig. 5(c). The position of the bend in Ω vs U corresponds to the value of U at which the double occupancy makes a jump [see Fig. 4(d)]. The other small jumps in P vs U are due to finite-size effects.

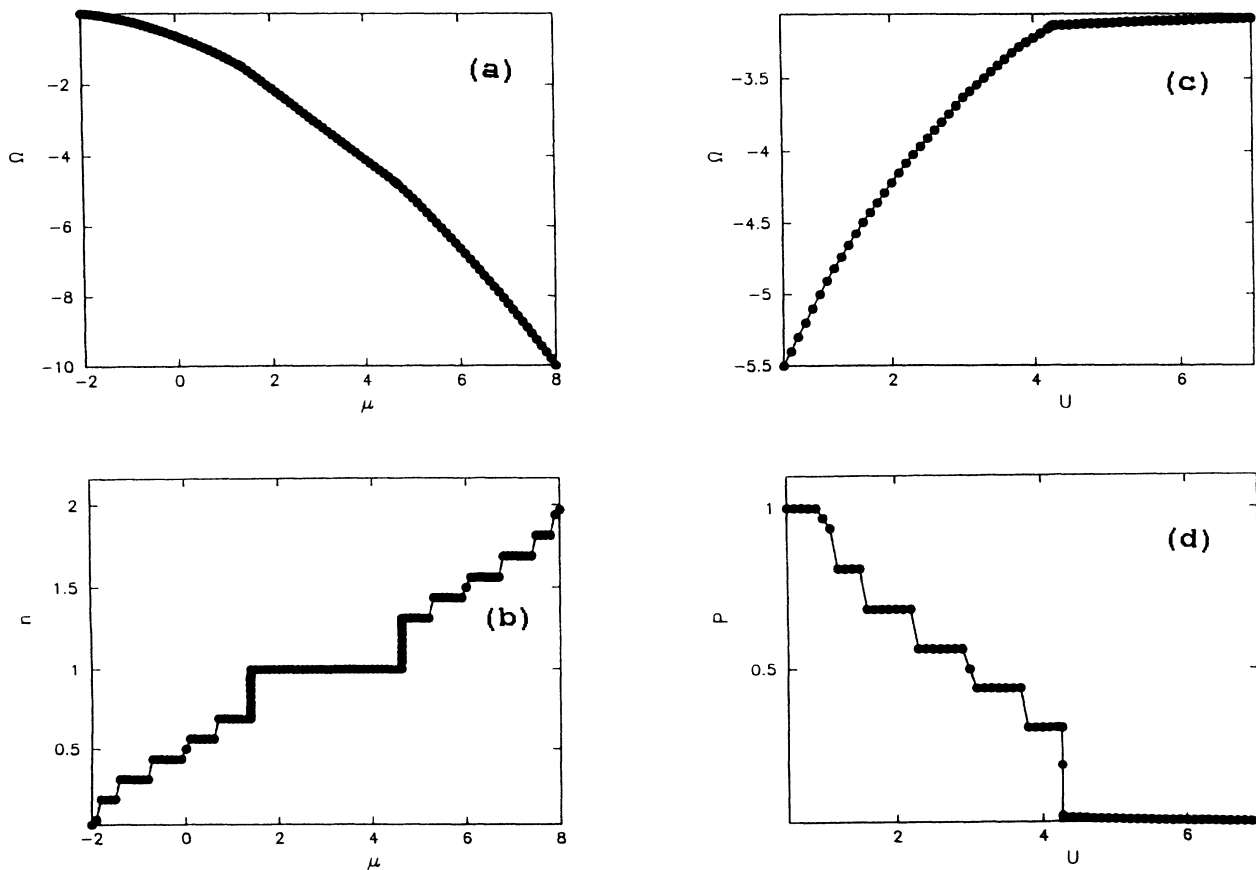


FIG. 5. Grand potential and first derivatives with respect to μ and U as a function of μ and U , respectively, for a ring of 16 sites for $t = 1, t' = 0.2, \gamma = 2$, and $\beta = 100$. (a) Ω as a function of μ for $U = 6$; (b) $n = -\partial\Omega/\partial\mu|_U$ as a function of μ for $U = 6$; (c) Ω as a function of U for $\mu = 3$; (d) $P = \partial\Omega/\partial U|_\mu$ as a function of U for $\mu = 3$. The lines are guides to the eye.

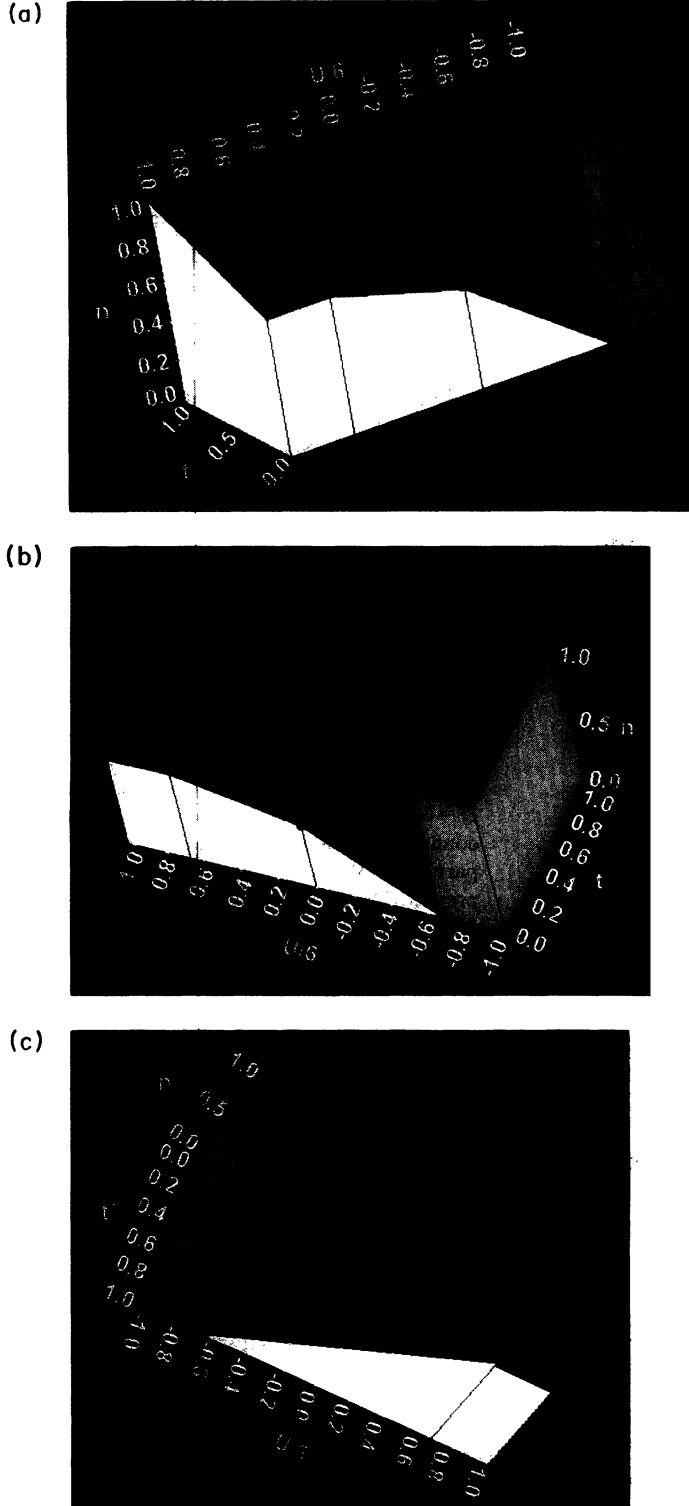


FIG. 6. Various views on the schematic ground-state (U, n, t') phase diagram for $\gamma=2$, $-1 \leq U/6 \leq 1$, $0 \leq n \leq 1$, and $0 \leq t' \leq t$ ($t=1$). The phase diagram for $1 < n \leq 2$ follows from the application of particle-hole symmetry. White: only mobile particles are present. Red: coexistence of two phases characterized by $D=0$ and a nearly perfect chessboard configuration of pairs of particles. Orange: coexistence of two phases characterized by $D=0$ and a nearly perfect chessboard configuration of unpaired mobile and immobile particles. Yellow: coexistence of a phase with no particles and a phase where pairs of particles are ordered into a nearly perfect chessboard configuration. Green: nearly perfect chessboard configuration of unpaired mobile and immobile particles. Violet: coexistence of two phases characterized by $D=0$ and $D=1$. Magenta: nearly perfect chessboard configuration of pairs of particles. Light blue: coexistence of a phase with no particles and a phase where all sites are occupied by pairs of particles. Blue tubes: regions without magnetic or charge ordering. The ground state is 2^{dL} times degenerate. Gray tube: coexistence of a phase characterized by $D=0$ and a phase for which the ground state is 2^{dL} times degenerate. (a) Top plane, $n=1$; front plane, $t'=0$; side plane, $U/6=1$. (b) Top plane, $n=1$; front plane, $t'=0$; side plane, $U/6=-1$. (c) Top plane, $n=1$; front plane, $t'=1$; side plane, $U/6=-1$. The thin lines are guides to the eye.

IV. SUMMARY

Various views on the schematic ground-state (U, n, t') phase diagram for $t=1$ derived on the basis of the model properties studied in this work are depicted in Figs. 6 and 7. We will consider the half-filled system first.

For $n=1$ [top plane in Figs. 6(a)–6(c)] and $t'=0$ the

system is insulating for $U \neq 0$ and conducting for $U=0$. For $U > 0$ the system is ordered into a nearly perfect chessboard configuration of unpaired mobile and immobile particles (green region) while for $U < 0$ the system is ordered into a nearly perfect chessboard configuration of pairs of particles (magenta region). The violet region in which the system is conducting and is phase separated

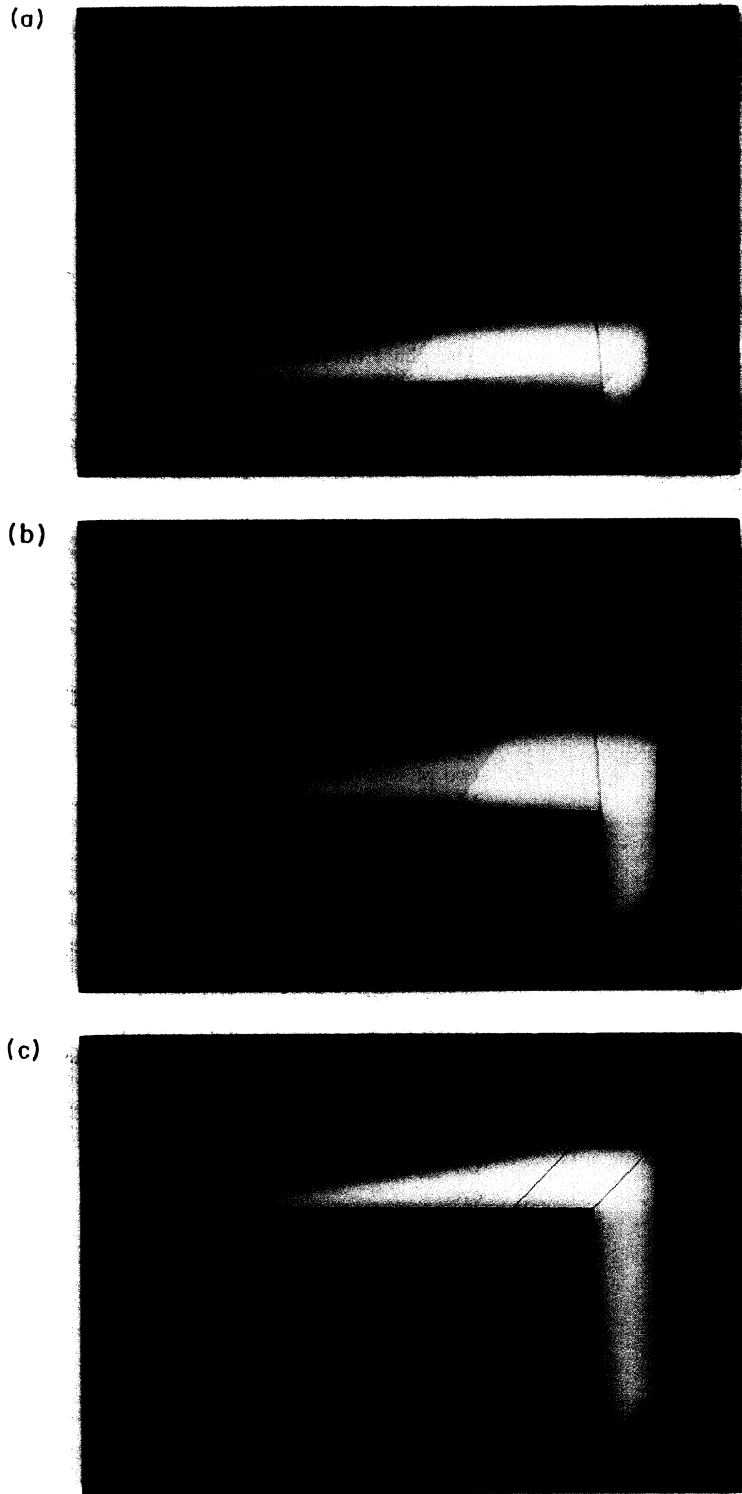


FIG. 7. Various slabs of the schematic ground-state (U, n, t') phase diagram for $\gamma=2$, $-1 \leq U/6 \leq 1$, $0 \leq n \leq 1$, and $0 \leq t' \leq t (t=1)$. The phase diagram for $1 < n \leq 2$ follows from the application of particle-hole symmetry. Blue: no particles are present. Yellow: coexistence of a phase with no particles and a phase where pairs of particles are ordered into a nearly perfect chessboard configuration. Red: coexistence of two phases characterized by $D=0$ and a nearly perfect chessboard configuration of pairs of particles. Violet: coexistence of two phases characterized by $D=0$ and $D=1$. Orange: coexistence of two phases characterized by $D=0$ and a nearly perfect chessboard configuration of unpaired mobile and immobile particles. White: only mobile particles are present. Light blue: coexistence of a phase with no particles and a phase where all sites are occupied by pairs of particles. Blue tubes: regions without magnetic or charge ordering. The ground state is 2^{dL} times degenerate. (a) Top plane, $t'=0.2$; (b) top plane, $t'=0.6$; (c) top plane, $t'=1$. The thin lines are guides to the eye.

into a phase with $D=0$ and a phase with $D=1$ increases with t' . The metal-insulator transition at the borders of the green or magenta and violet regions is discontinuous. For $t'=1$ the magenta and green regions are replaced by regions where the system is insulating and has neither magnetic nor charge ordering (blue tubes). For $t'=1$ the metal-insulator transition occurs at $U=4$ and is continuous.

Away from half-filling it follows from Figs. 6(a) and 6(b) that for $t'=0$ (front plane) there are four distinct regions: For $U \leq -4$ and for all $n < 1$ the system is phase separated into a phase with no particles and a phase where pairs of particles are ordered into a nearly perfect chessboard configuration (yellow region). In this region the system is insulating. For $-4 < U < 0$, there are only mobile particles in the system up to some filling n (white

region) and above this filling there is coexistence between a phase with only mobile particles and a phase where pairs of particles are ordered into a nearly perfect chessboard configuration (red region). For $U=0$, there are no immobile particles in the system up to some filling n (white region) and above this filling both (free) mobile and (free) immobile particles are present. The system separates into a phase characterized by $D=0$ and a phase for which the ground state is 2^{dL} times degenerate (gray tube). For $U > 0$, there are only mobile particles in the system up to some filling n (white region) but, in contrast to the $-4 < U < 0$ case, beyond this filling the system separates into a phase with only mobile particles and a phase where unpaired mobile and immobile particles are ordered into a nearly perfect chessboard configuration (orange region). For $U > -4$ and $n < 1$ the system is conducting.

For $t'=1$ [front plane in Fig. 6(c)] and $n < 1$ there are three distinct regions: For $U \leq -4$ and for all $n < 1$ there is coexistence between a phase with no particles and a

phase with 2^{dL} particles (light-blue region). Just as for $t'=0$, in this region the system is insulating. For $U > -4$, there are only mobile particles in the system up to some filling n (white region) and above this filling the system phase separates into a phase with $D=0$ and a phase with $D=1$ (violet region). For $U > -4$ and $n < 1$ the system is conducting. Information on the (U, n, t') phase diagram for $t' \neq 0, 1$ is provided by Fig. 7, where we show different views of the interior of the phase diagram.

ACKNOWLEDGMENTS

We would like to thank F. F. Assaad for stimulating discussions and useful suggestions. This work is partially supported by the Stichting voor Fundamenteel Onderzoek der Materie (FOM), which is financially supported by the Nederlandse Organisatie voor Wetenschappelijk Onderzoek (NWO), and a supercomputer grant of the Stichting Nationale Computer Faciliteiten (NCF).

-
- [1] L. E. Reichl, *A Modern Course in Statistical Physics* (Edward Arnold, London, 1980).
 - [2] M. Suzuki, *Prog. Theor. Phys.* **56**, 1454 (1976).
 - [3] R. J. Elliot, P. Pfeuty, and C. Wood, *Phys. Rev. Lett.* **25**, 443 (1970).
 - [4] M. Suzuki, *Prog. Theor. Phys.* **46**, 1337 (1971).
 - [5] O. F. de Alcantara Bonfim and T. Schneider, *Phys. Rev. B* **30**, 1629 (1984).
 - [6] M. E. Fisher, *Rev. Mod. Phys.* **46**, 597 (1974).
 - [7] J. Hubbard, *Proc. R. Soc. London Ser. A* **281**, 401 (1964).
 - [8] T. Kennedy and E. H. Lieb, *Physica A* **138**, 320 (1986).
 - [9] J. Jedrzejewsky, J. Lach, and R. Lyzwa, *Physica A* **154**, 529 (1989).
 - [10] L. M. Falicov and J. C. Kimball, *Phys. Rev. Lett.* **22**, 997 (1969).
 - [11] K. Michielsen, *Phys. Rev. B* **50**, 4283 (1994).
 - [12] A. Montorsi and M. Rasetti, *Phys. Rev. Lett.* **66**, 1383 (1991).
 - [13] K. Michielsen, *Int. J. Mod. Phys. B* **7**, 2571 (1993).
 - [14] K. Michielsen, H. De Raedt, and T. Schneider, *Phys. Rev. Lett.* **68**, 1410 (1992).
 - [15] J. Hubbard, *Proc. R. Soc. London Ser. A* **276**, 238 (1963).
 - [16] M. C. Gutzwiller, *Phys. Rev. Lett.* **10**, 159 (1963).
 - [17] U. Brandt and R. Schmidt, *Z. Phys. B* **67**, 43 (1986).
 - [18] J. E. Hirsch, *Physica C* **158**, 326 (1989).
 - [19] H. De Raedt and W. von der Linden, in *The Monte Carlo Method in Condensed Matter Physics*, edited by K. Binder, Topics in Applied Physics Vol. 71 (Springer, Berlin, 1992).
 - [20] P. de Vries, K. Michielsen, and H. De Raedt, *Z. Phys. B* **92**, 353 (1993).

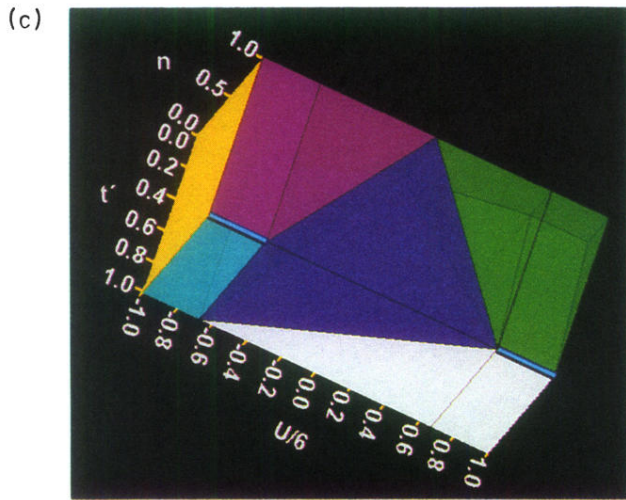
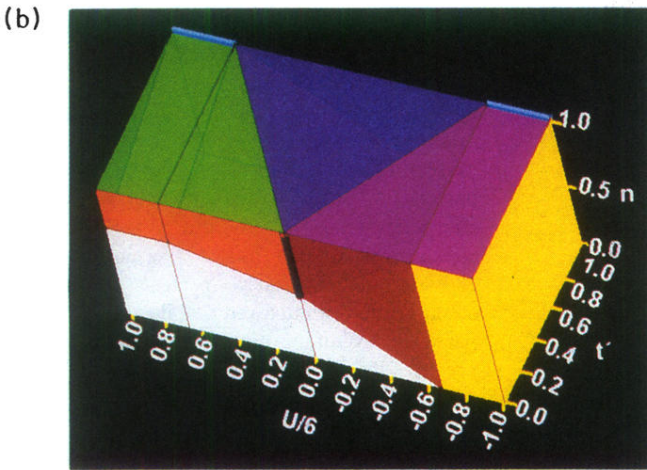
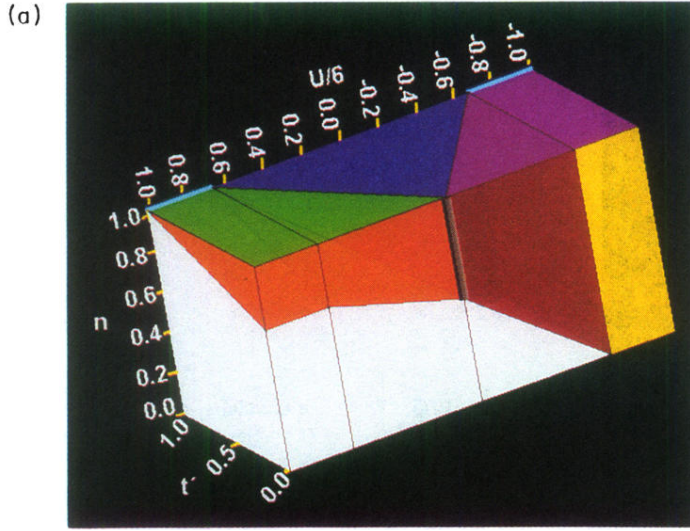


FIG. 6. Various views on the schematic ground-state (U, n, t') phase diagram for $\gamma=2$, $-1 \leq U/6 \leq 1$, $0 \leq n \leq 1$, and $0 \leq t' \leq t$ ($t=1$). The phase diagram for $1 < n \leq 2$ follows from the application of particle-hole symmetry. White: only mobile particles are present. Red: coexistence of two phases characterized by $D=0$ and a nearly perfect chessboard configuration of pairs of particles. Orange: coexistence of two phases characterized by $D=0$ and a nearly perfect chessboard configuration of unpaired mobile and immobile particles. Yellow: coexistence of a phase with no particles and a phase where pairs of particles are ordered into a nearly perfect chessboard configuration. Green: nearly perfect chessboard configuration of unpaired mobile and immobile particles. Violet: coexistence of two phases characterized by $D=0$ and $D=1$. Magenta: nearly perfect chessboard configuration of pairs of particles. Light blue: coexistence of a phase with no particles and a phase where all sites are occupied by pairs of particles. Blue tubes: regions without magnetic or charge ordering. The ground state is 2^{dL} times degenerate. Gray tube: coexistence of a phase characterized by $D=0$ and a phase for which the ground state is 2^{dL} times degenerate. (a) Top plane, $n=1$; front plane, $t'=0$; side plane, $U/6=1$. (b) Top plane, $n=1$; front plane, $t'=0$; side plane, $U/6=-1$. (c) Top plane, $n=1$; front plane, $t'=1$; side plane, $U/6=-1$. The thin lines are guides to the eye.

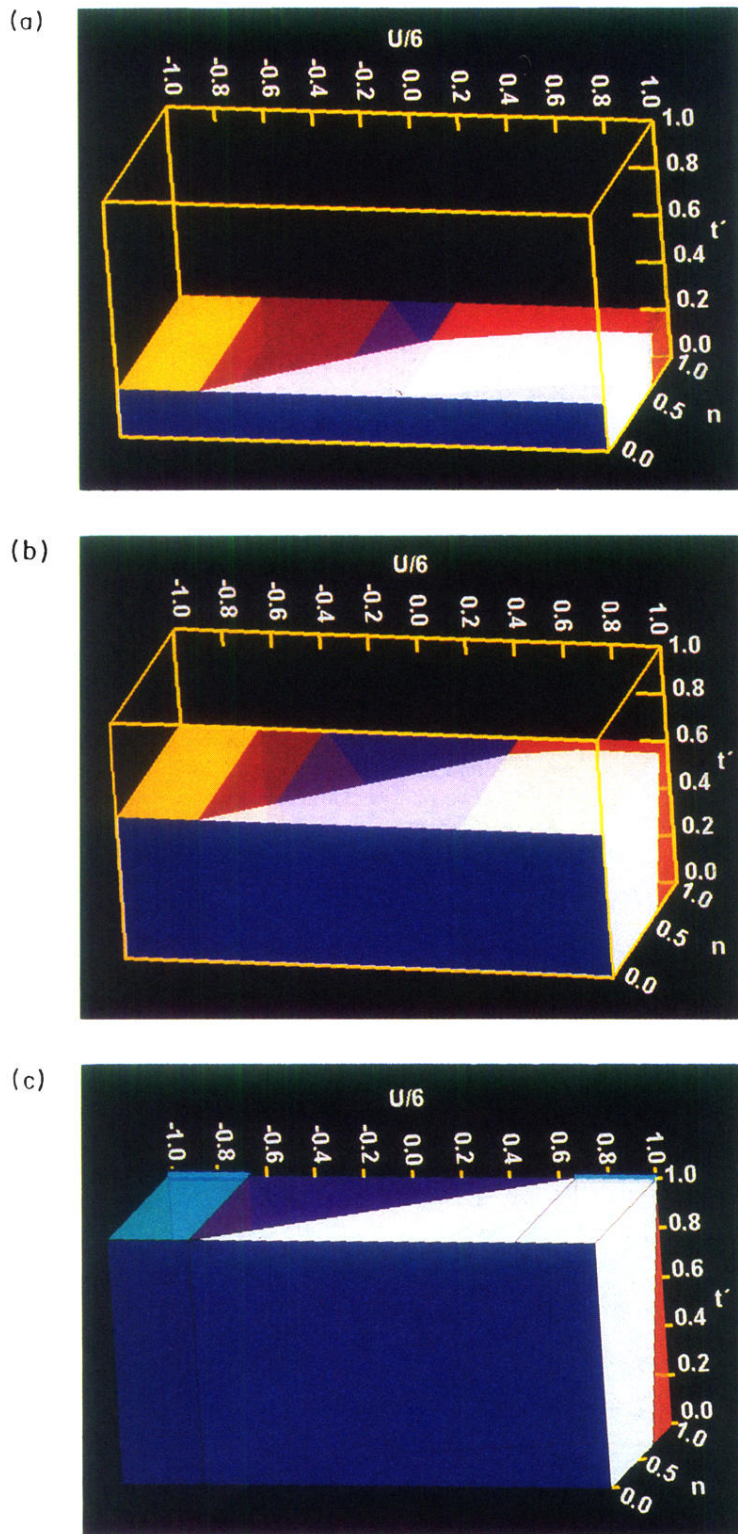


FIG. 7. Various slabs of the schematic ground-state (U, n, t') phase diagram for $\gamma=2$, $-1 \leq U/6 \leq 1$, $0 \leq n \leq 1$, and $0 \leq t' \leq t (t=1)$. The phase diagram for $1 < n \leq 2$ follows from the application of particle-hole symmetry. Blue: no particles are present. Yellow: coexistence of a phase with no particles and a phase where pairs of particles are ordered into a nearly perfect chessboard configuration. Red: coexistence of two phases characterized by $D=0$ and a nearly perfect chessboard configuration of pairs of particles. Violet: coexistence of two phases characterized by $D=0$ and $D=1$. Orange: coexistence of two phases characterized by $D=0$ and a nearly perfect chessboard configuration of unpaired mobile and immobile particles. White: only mobile particles are present. Light blue: coexistence of a phase with no particles and a phase where all sites are occupied by pairs of particles. Blue tubes: regions without magnetic or charge ordering. The ground state is 2^{dL} times degenerate. (a) Top plane, $t'=0.2$; (b) top plane, $t'=0.6$; (c) top plane, $t'=1$. The thin lines are guides to the eye.